

# Visible-Active SnS<sub>2</sub>/g-C<sub>3</sub>N<sub>4</sub> Photocatalyst for Effective Reactive Orange 16 Dye Removal

Wipawee O-in, Kanokon Srijan & Uraiwan Sirimahachai

Center of Excellence for Innovation in Chemistry, Division of Physical Chemistry,  
Faculty of Science, Prince of Songkla University, Hatyai, Songkla, 90110, Thailand

*uraiwan.s@psu.ac.th*

## ABSTRACT

One-pot synthesis of SnS<sub>2</sub>/g-C<sub>3</sub>N<sub>4</sub> composite by thermal polycondensation method. Tin (IV) chloride and thiourea have been used as precursors for synthesis of SnS<sub>2</sub>/g-C<sub>3</sub>N<sub>4</sub> composite with varied SnS<sub>2</sub> ratio. All samples were characterized by X-ray diffraction spectroscopy (XRD), field emission scanning electron microscope and energy-dispersive X-ray-spectroscopy (FE-SEM and EDX), UV-visible diffuse reflectance spectroscopy (UV-Vis DRS), and fourier-transform infrared spectroscopy (FTIR). The photocatalytic performance of all samples can be monitored by photodegradation of reactive orange 16 (RO16) under visible light irradiation. The best photocatalyst was 1%SnS<sub>2</sub>/g-C<sub>3</sub>N<sub>4</sub> which showed 87.19% ( $k_{app} = 0.0640 \text{ min}^{-1}$ ) degradation of RO16 within 30 min. The major reactive species was  $\cdot\text{O}_2^-$ .

**Key Words:** Photocatalysis; g-C<sub>3</sub>N<sub>4</sub>; SnS<sub>2</sub>; heterojunction.

## 1. INTRODUCTION

One of the important industrial pollution is organic pollution because its high toxicity, stable, and difficult degradation. Thus, excellent methods to eliminate of pollution from water need to be investigated. Elimination of organic compounds which had many different methods such as air stripping, precipitation, reverse osmosis, adsorption, ultra-filtration, and flocculation were developed (Hussain et al., 2017). The photocatalysis has been attention for the decomposition of organic pollution. It had many advantages like nontoxic to the environment, producing CO<sub>2</sub>, H<sub>2</sub>O and other nontoxic substances as the final products, high degradation rate, high efficiency (Zhao et al., 2018) and reaction activity can be stopped at any time (Pan et al., 2019).

Among the semiconductor materials, graphite-like or graphitic carbon nitride (g-C<sub>3</sub>N<sub>4</sub>) was metal-free layered polymer semiconductor which had more attention due to it had appropriate band gap (2.7 eV) structure for visible light adsorption, thermal stability, low price, easy synthesis method as prepared by direct thermal pyrolysis of suitable precursors, easy of large-scale preparation, non-toxicity and high chemical stability (Feng et al., 2016). The g-C<sub>3</sub>N<sub>4</sub> had many applications such as detoxification of wastewater, CO<sub>2</sub> reduction, hydrogen/oxygen evolution through water splitting, electroactive materials for batteries, bioimaging and sensor (Yuan et al., 2016). However, the photocatalytic process of g-C<sub>3</sub>N<sub>4</sub> was limited by the high recombination rate of the photoelectrons and holes and low specific surface area. Therefore, to solve the problem, many methods were used such as nonmetal or metal (C, P, B, and Fe, etc.) doping, noble metal (Au, Pt, and Ag, etc.) nanoparticles deposition, preparation of porous g-C<sub>3</sub>N<sub>4</sub> and designing heterojunction composite (TiO<sub>2</sub>/g-C<sub>3</sub>N<sub>4</sub>, Ag<sub>3</sub>PO<sub>4</sub>/g-C<sub>3</sub>N<sub>4</sub>, ZnO/g-C<sub>3</sub>N<sub>4</sub>, and Bi<sub>2</sub>WO<sub>6</sub>/g-C<sub>3</sub>N<sub>4</sub>, etc.) (Li et al., 2016).

Metal sulfide such as Molybdenum sulfide (MoS<sub>2</sub>) has been revealed to be excellent co-catalyst (Li et al., 2016), Zinc sulfide (ZnS) has some advantages as a good photocatalyst with eco-friendliness,

excellent stability, and low cost (Yan et al., 2017), Copper sulfide (CuS) was catalyst that had properties in a broad range of environmental application (Khan et al., 2018), Cadmium sulfide (CdS) was widely used due to it was a sensitizing agent to enhance the visible light response range of wide band gap semiconductors (Li et al., 2019), Bismuth sulfide ( $\text{Bi}_2\text{S}_3$ ) had a suitable band gap, a reasonable photon conversion efficiency of about 5% and a non-toxic (Hu et al., 2019), Tin sulfide (SnS) has a narrow band-gap of 1.3 eV and holds the typical features of low cost, earth element abundance, chemical inertness, and wide spectral response ranging from visible to near infrared region (Jia et al., 2020). Tin disulfide ( $\text{SnS}_2$ ) was important semiconductor with a band gap energy about 2.18-2.44 eV that used widely studied such as gas sensing, photocatalysis, solar cell, and anode materials. Moreover,  $\text{SnS}_2$  had various morphologies like nanotubes, nanorods, nanosheets, and nanoflowers which alternate band gap energies controlling (Chen et al., 2016). This was the one of interesting alternative for doping with  $\text{g-C}_3\text{N}_4$ .

In this work, Tin (IV) sulfide ( $\text{SnS}_2$ ) has been synthesized and fabricated on  $\text{g-C}_3\text{N}_4$  via one-step thermal polycondensation method. The photocatalysis results indicated that this composite could reduce the electron-hole recombination rates of the photogenerated charge carriers of  $\text{g-C}_3\text{N}_4$  to improve photocatalytic performance of organic dye degradation.

## 2. METHODOLOGY

### 2.1. Synthesis of $\text{SnS}_2/\text{gC}_3\text{N}_4$

One-pot synthesis of  $\text{SnS}_2/\text{gC}_3\text{N}_4$  was performed by thermal polycondensation method as follow; 10 g of Thiourea and restricted amount of  $\text{SnCl}_4 \cdot 5\text{H}_2\text{O}$  were added into beaker following with 2 mL of distilled water and mixed. Then, the mixture was heated in an oven at 80 °C for 1 h. Finally, dried powder was calcined at 550 °C for 2 h under atmosphere. The % weight ratio of  $\text{SnCl}_4 \cdot 5\text{H}_2\text{O}$  and thiourea was varied and assigned as 1% and 2%  $\text{SnS}_2/\text{g-C}_3\text{N}_4$ . Pure  $\text{g-C}_3\text{N}_4$  from thiourea was also synthesized without adding  $\text{SnCl}_4 \cdot 5\text{H}_2\text{O}$ .

### 2.2. Photocatalytic studied

The photocatalytic performance of  $\text{SnS}_2/\text{gC}_3\text{N}_4$  was determined by monitoring the degradation of reactive orange16 (RO16, pollutant dye model) under visible light irradiation (55W Xe-lamp). In each experiment, 0.1500 g of  $\text{SnS}_2/\text{gC}_3\text{N}_4$  photocatalyst was added into 150 mL of RO16 solution (10ppm). Then magnetically stirred in the dark for 30 min was performed to reach an adsorption-desorption equilibrium. The solution was subsequently irradiated at room temperature. The 3 mL of solution was withdrawn every 15 min interval until 120 min. In order to determine the concentration of RO16 dye, UV-Vis spectrophotometer was used to determine the absorbance at  $\lambda_{\text{max}}$  of 493 nm. The photocatalytic mechanism of synthesized photocatalyst over RO16 can be investigated by adding radical scavengers in reaction and monitoring the absorbance of RO16.

## 3. RESULTS AND DISCUSSION

### 3.1. Synthesis and characterization

One-pot synthesis of all photocatalysts were successfully performed via thermal polycondensation method. Phase of all samples were confirmed by X-ray diffraction spectroscopy as shown in Figure 1(a) The diffraction peak around 13.0 and 27.0 degree were indexed as (1 0 0) and (0 0 2) diffraction plane of  $\text{g-C}_3\text{N}_4$  (JCPDS No.87-1526), respectively. These two peaks corresponding to the triazine unit and the interlayer stacking of aromatic units of  $\text{g-C}_3\text{N}_4$ , respectively (Sundaram et al., 2018; Solehudin et al., 2020), which confirmed the existing of  $\text{g-C}_3\text{N}_4$ . The intensity of peaks decreased as the increasing ratio of  $\text{SnS}_2$  because the polycondensation process of  $\text{g-C}_3\text{N}_4$  might be interfered by  $\text{SnS}_2$ . In Figure 1(b), FTIR spectra of all samples have been used to confirm the  $\text{g-C}_3\text{N}_4$  structure. These peaks at wavenumber around 810 accords with characteristic breathing mode of triazine units. The peaks around 1200-1700  $\text{cm}^{-1}$  can attributed to stretching vibration C-N heterocyclic. The stretching vibration of N-H bonds or  $\text{NH}_2$  groups of  $\text{g-C}_3\text{N}_4$  was observed at 3000-3400  $\text{cm}^{-1}$  (Sundaram et al., 2018; Zhu et al.,

2015). The DRS spectra and Talc plots (Figure 1(c) and (d)) revealed that all samples can absorb visible light then the photocatalytic activity of all samples can be activated under visible light irradiation.

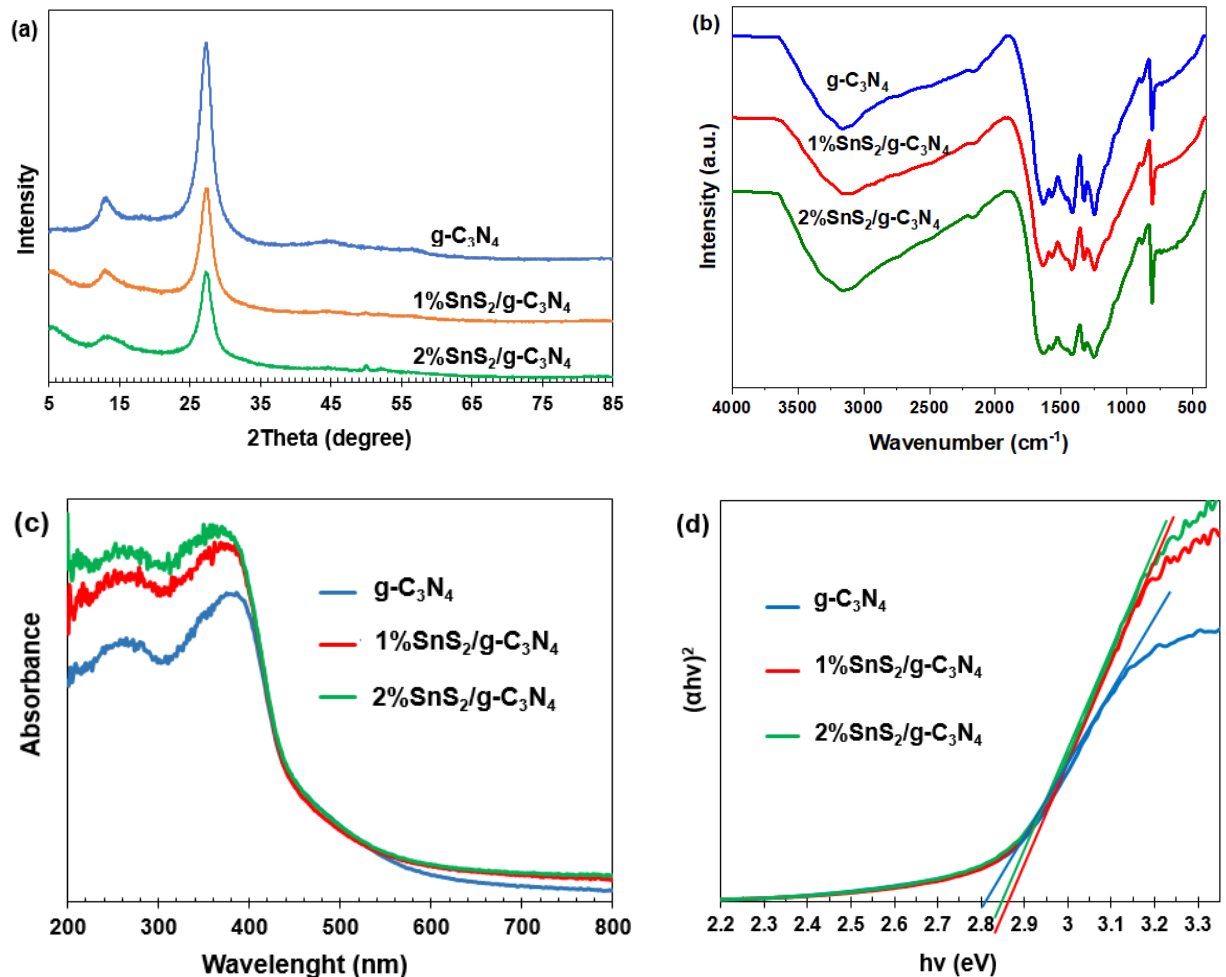


Figure 1: XRD patterns (a), FTIR spectra (b), DRS spectra (c) and Talc plots of synthesized photocatalysts (d)

The morphology and elements of 1%SnS<sub>2</sub>/g-C<sub>3</sub>N<sub>4</sub> were investigated by FE-SEM and EDS techniques as shown in Figure 2. In Fig 2a, 1%SnS<sub>2</sub>/g-C<sub>3</sub>N<sub>4</sub> was consisted of sheets morphology and slight porosity on the sample surface which can improve the photocatalytic activity. Furthermore, EDS mapping spectra as shown in Fig 2b. The elements of 1%SnS<sub>2</sub>/g-C<sub>3</sub>N<sub>4</sub> was composed with C, N, Sn and S. These elements were clearly demonstrated distribution over 1%SnS<sub>2</sub>/g-C<sub>3</sub>N<sub>4</sub> with a percentage of 33.8, 62.1, 1.2, and 0.3 % for C, N, Sn, and S, respectively.

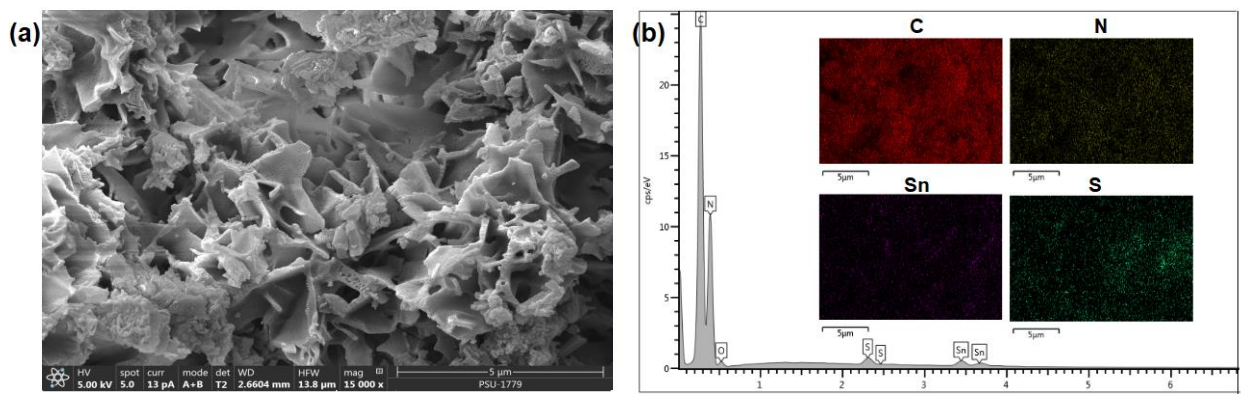


Figure 2: SEM-EDS mapping of 1%SnS<sub>2</sub>/g-C<sub>3</sub>N<sub>4</sub> photocatalyst

### 3.2. Photocatalytic activity

The photocatalytic performance of all samples was studied by monitoring the degradation of RO16 dye under visible light illumination as shown in Figure 3(a) and Table 1.

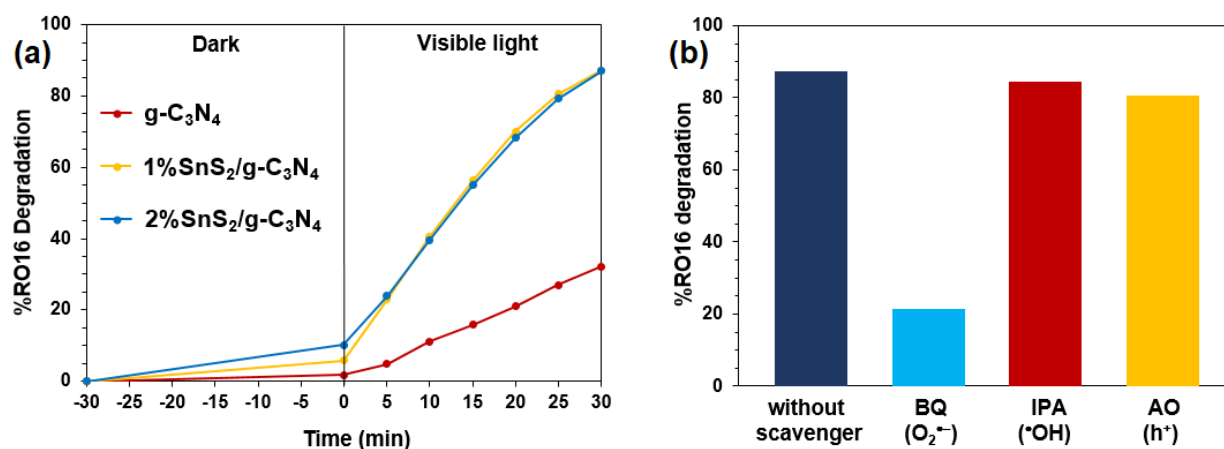


Figure 3: Photocatalytic degradation of RO16 (a) and the presence of different scavengers over the photocatalytic activity of 1%SnS<sub>2</sub>/g-C<sub>3</sub>N<sub>4</sub> (b)

Graphitic carbon nitride (g-C<sub>3</sub>N<sub>4</sub>) fabricated with SnS<sub>2</sub> show greater photocatalytic efficiency than that in pure g-C<sub>3</sub>N<sub>4</sub>. This might come from the creation of heterojunction between SnS<sub>2</sub> and g-C<sub>3</sub>N<sub>4</sub> results in reducing the electron-hole pair recombination. The  $k_{app}$  values have been determined as indicated in Table 1. It can be concluded that 1%SnS<sub>2</sub>/g-C<sub>3</sub>N<sub>4</sub> is the best photocatalyst in this work (Table 1).

Table 2 %RO16 degradation and  $k_{app}$  value

photocatalyst	%RO16 degradation	$k_{app}$ (min <sup>-1</sup> )
g-C <sub>3</sub> N <sub>4</sub>	32.18%	0.0124
1%SnS <sub>2</sub> /g-C <sub>3</sub> N <sub>4</sub>	87.19%	0.0640
2%SnS <sub>2</sub> /g-C <sub>3</sub> N <sub>4</sub>	86.99%	0.0623

Benzoquinone (BQ), ammonium oxalate (AO), and isopropyl alcohol (IPA) have been used as radical scavenger for O<sub>2</sub><sup>-</sup> (superoxide radical), h<sup>+</sup> (hole), and •OH (hydroxyl radical), respectively. The %RO16 degradation after adding different scavengers into system of 1%SnS<sub>2</sub>/g-C<sub>3</sub>N<sub>4</sub> was revealed in Fig 3(b). The BQ clearly inhibited RO16 dye degradation. Therefore, the O<sub>2</sub><sup>-</sup> was the major reactive species of RO16 dye degradation in this work.

### 4. CONCLUSION

One-pot synthesis of SnS<sub>2</sub>/g-C<sub>3</sub>N<sub>4</sub> was successfully prepared via thermal polycondensation method. All characterization techniques confirmed the existing of g-C<sub>3</sub>N<sub>4</sub>. The FE-SEM and EDS techniques ensured the existing of SnS<sub>2</sub>. The best photocatalyst in this work was 1%SnS<sub>2</sub>/g-C<sub>3</sub>N<sub>4</sub> with 87.19% RO16 degradation ( $k_{app} = 0.0640$  min<sup>-1</sup>) within 30 min under visible light irradiation. It can be conclude that modified SnS<sub>2</sub> onto g-C<sub>3</sub>N<sub>4</sub> could improve the photodegradation efficiency of g-C<sub>3</sub>N<sub>4</sub> and resolve the problem of organic pollutants in environment.

### ACKNOWLEDGEMENTS

This research was supported by Graduate School Scholarship and Division of Physical Science, Faculty of Science, Prince of Songkla University. Financial support from the Center of Excellence for Innovation in Chemistry (PERCH-CIC), Ministry of Higher Education, Science, Research, and Innovation is gratefully acknowledged.

## REFERENCES

- Li, J., Liu, E., Ma, Y., Hu, X., Wan, J., Sun, L., et al. (2016). Synthesis of MoS<sub>2</sub>/g-C<sub>3</sub>N<sub>4</sub> nanosheets as 2D heterojunction photocatalysts with enhanced visible light activity. *Applied Surface Science*, 364, 694-702.
- Chen, L., Chen, M., Jiang, D., & Xie, J. (2016). A facile strategy for SnS<sub>2</sub>/g-C<sub>3</sub>N<sub>4</sub> heterojunction composite and the mechanism in photocatalytic degradation of MO. *Journal of Molecular Catalysis A: Chemical*, 425, 174-182.
- Feng, J., Chen, T., Liu, S., Zhou, Q., Ren, Y., Lv, Y., et al. (2016). Improvement of g-C<sub>3</sub>N<sub>4</sub> photocatalytic properties using the Hummers method. *Journal of Colloid and Interface Science*, 479, 1-6.
- Yuan, X., Zhou, C., Jin, Y., Jing, Q., Yang, Y., Shen, X., et al. (2016). Facile synthesis of 3D porous thermally exfoliated g-C<sub>3</sub>N<sub>4</sub> nanosheet with enhanced photocatalytic degradation of organic dye. *Journal of Colloid and Interface Science*, 468, 211-219.
- Hussain, W., Badshah, A., Hussain, R. A., Imtiaz ud, D., Aleem, M. A., Bahadur, A., et al. (2017). Photocatalytic applications of Cr<sub>2</sub>S<sub>3</sub> synthesized from single and multi-source precursors. *Materials Chemistry and Physics*, 194, 345-355.
- Yan, J., Fan, Y., Lian, J., Zhao, Y., Xu, Y., Gu, J., et al. (2017). Kinetics and mechanism of enhanced photocatalytic activity employing ZnS nanospheres/graphene-like C<sub>3</sub>N<sub>4</sub>. *Molecular Catalysis*, 438, 103-112.
- Khan, A., Alam, U., Raza, W., Bahnemann, D., & Muneer, M. (2018). One-pot, self-assembled hydrothermal synthesis of 3D flower-like CuS/g-C<sub>3</sub>N<sub>4</sub> composite with enhanced photocatalytic activity under visible-light irradiation. *Journal of Physics and Chemistry of Solids*, 115, 59-68.
- Zhao, W., Wei, Z., Zhang, L., Wu, X., & Wang, X. (2018). Cr doped SnS<sub>2</sub> nanoflowers: Preparation, characterization and photocatalytic decolorization. *Materials Science in Semiconductor Processing*, 88, 173-180.
- Pan, H., Xie, H., Chen, G., Xu, N., Wang, M., & Fakhri, A. (2020). Cr<sub>2</sub>S<sub>3</sub>-Co<sub>3</sub>O<sub>4</sub> on polyethylene glycol-chitosan nanocomposites with enhanced ultraviolet light photocatalysis activity, antibacterial and antioxidant studies. *International Journal of Biological Macromolecules*, 148, 608-614.
- Jia, T., Fu, F., Li, J., Deng, Z., Long, F., Yu, D., et al. (2020). Rational construction of direct Z-scheme SnS/g-C<sub>3</sub>N<sub>4</sub> hybrid photocatalyst for significant enhancement of visible-light photocatalytic activity. *Applied Surface Science*, 499, 143941.
- Hu, T., Dai, K., Zhang, J., Zhu, G., & Liang, C. (2019). One-pot synthesis of step-scheme Bi<sub>2</sub>S<sub>3</sub>/porous g-C<sub>3</sub>N<sub>4</sub> heterostructure for enhanced photocatalytic performance. *Materials Letters*, 257, 126740.
- Solehudin, M., Sirimahachai, U., Ali, G. A. M., Chong, K. F., & Wongnawa, S. (2020). One-pot synthesis of isotype heterojunction g-C<sub>3</sub>N<sub>4</sub>-MU photocatalyst for effective tetracycline hydrochloride antibiotic and reactive orange 16 dye removal. *Advanced Powder Technology*, 31(5), 1891-1902.
- Sundaram, I. M., Kalimuthu, S., & Gomathi priya, P. (2018). Metal-free heterojunction of graphitic carbon nitride composite with superior and stable visible-light active photocatalysis. *Materials Chemistry and Physics*, 204, 243-250.
- Zhu, Z., Lu, Z., Zhao, X., Yan, Y., Shi, W., Wang, D., et al. (2015). Surface imprinting of a g-C<sub>3</sub>N<sub>4</sub> photocatalyst for enhanced photocatalytic activity and selectivity towards photodegradation of 2-mercaptobenzothiazole. [10.1039/C5RA06209H]. *RSC Advances*, 5(51), 40726-40736.